

# The theory and application of Navier-Stokeslets (NSlets)

Cite as: Phys. Fluids 31, 107103 (2019); <https://doi.org/10.1063/1.5119331>

Submitted: 10 July 2019 . Accepted: 12 September 2019 . Published Online: 01 October 2019

E. Chadwick 



View Online



Export Citation



CrossMark



Scilight Highlights of the best new research in the physical sciences

[LEARN MORE!](#)



# The theory and application of Navier-Stokeslets (NSlets)

Cite as: Phys. Fluids 31, 107103 (2019); doi: 10.1063/1.5119331

Submitted: 10 July 2019 • Accepted: 12 September 2019 •

Published Online: 1 October 2019



View Online



Export Citation



CrossMark

E. Chadwick<sup>a)</sup> 

## AFFILIATIONS

Mathematics, University of Salford, Salford M54WT, United Kingdom

<sup>a)</sup>Electronic mail: [e.a.chadwick@salford.ac.uk](mailto:e.a.chadwick@salford.ac.uk)

## ABSTRACT

Consider a closed body moving in an unbounded fluid that decays to rest in the far-field and governed by the incompressible Navier-Stokes equations. By considering a translating reference frame, this is equivalent to a uniform flow past the body. A velocity representation is given as an integral distribution of Green's functions of the Navier-Stokes equations which we shall call NSlets. The strength of the NSlets is the same as the force distribution over the body boundary. An expansion for the NSlet is given with the leading-order term being the Oseenlet. To test the theory, the following three two-dimensional steady flow benchmark applications are considered. First, consider uniform flow past a circular cylinder for three cases: low Reynolds number, high Reynolds number, and also intermediate Reynolds numbers at values 26 and 36. These values are chosen because the flow is still steady and has not yet become unsteady. For the low Reynolds number, approximate the NSlet by the leading order Oseenlet term. For the high Reynolds number, approximate the NSlet by the Eulerlet which is the leading order Oseenlet in the high Reynolds number limit. For the intermediate Reynolds numbers, approximate the NSlet by an Eulerlet close to its origin and an Oseenlet further away. Second, consider uniform flow past a slender body with elliptical cross section with Reynolds number  $Re \sim 10^6$  and approximate the NSlet by the Eulerlet. Finally, consider the Blasius problem of uniform flow past a semi-infinite flat plate and consider the first three terms in the NSlet approximation.

Published under license by AIP Publishing. <https://doi.org/10.1063/1.5119331>

## I. INTRODUCTION

A Boundary Integral velocity representation is derived for the Navier-Stokes equations in terms of their Green's functions, called NSlets, for a body in an exterior-domain uniform flow. This result is already known for the steady case,<sup>1</sup> where it is assumed that the boundary integral representations around the fluid point and the body can be represented by domain integrations involving Dirac delta functions. In this paper, these assumptions shall not be made and, instead, the Boundary Integral representations shall be evaluated directly. Furthermore, the representation is extended to include time dependent as well as steady flow.

The result is a generalization of existing results in the literature for Stokes,<sup>2,3</sup> Oseen,<sup>4</sup> and Euler<sup>5</sup> models. These represent the flow by an integral distribution over the body boundary of their respective Green's functions which have a strength given by the force distribution. In the low Reynolds number limit, the NSlet tends to the Stokeslet; in the high Reynolds number limit, the NSlet tends to the Eulerlet, and in the far-field, the NSlet tends to the Oseenlet. In this

way, the new formulation is seen to reduce to existing formulations. For the Stokes and Oseen flow, the boundary integral representation in terms of Stokeslets and Oseenlets, respectively, is well-known in the literature as the equations are linear.<sup>2-4</sup> However, the result for Euler flow by using Eulerlets is significant as it gives a Green's integral representation for the velocity of the nonlinear Euler equations.<sup>5</sup> A theoretical argument was then given for Navier-Stokes flow by using NSlets,<sup>1</sup> but this argument assumed the use of Dirac delta function representations of the domain integrations rather than the boundary integrations and was also restricted to the steady case only.

In the present paper, this assumption is not made, and instead, we look to evaluate the boundary integrals rather than the delta function domain integrals in the Green's integral representation. To evaluate the integration around the fluid point, we note that a moving reference frame translating with the velocity of the fluid point will in the vicinity of the point have a vanishingly small fluid velocity and so will be represented by a linear Stokes flow. The nonlinearity in the Eulerian Navier-Stokes description begins

to disappear and approach the Lagrangian representation following a fluid particle in the vicinity of the point where the Lagrangian and Eulerian representations approach each other. Similarly, the far-field integration will be represented by an Oseen flow. This means that over both these integrals, the flow becomes linear and the nonlinear quadratic variation in the Navier-Stokes equations becomes negligible; in this way, the integrals may be subsequently evaluated. This is also checked by determining the order of contribution from the nonlinear variation and demonstrating that it is vanishingly small in the limit. Furthermore, the nonlinear contribution in the Green's integral representation is shown to be represented by a potential defined by a line integration over a radial spoke emanating from the fluid point. By considering the interior as well as exterior problem, we see that this potential is continuous over the body domain boundary as we cross from the exterior to the interior domain. Consequently, the nonlinear contributions from the exterior and the interior domains cancel, yielding a velocity representation by a linear integral distribution of NSlets only.

We give a representation of the NSlet by an infinite series expansion with the first term being the Oseenlet. In this way, the theory is tested on three benchmark problems.

First, consider uniform flow past a circular cylinder for three cases: low, high, and intermediate Reynolds numbers. For the low Reynolds number approaching unity, it is shown that the drag coefficient is closer to the experiment than the matched asymptotic method of Kaplun and Lagerstrom<sup>6</sup> where Kaplun's result is given by Yano and Kieda.<sup>7</sup> For the high Reynolds number, the NSlet is approximated by the Eulerlet which is the leading order Oseenlet in the high Reynolds number limit; refer to the results of Chadwick<sup>5</sup> which show good agreement with the experiment for laminar and turbulent flows. There have been several recent studies on flow past cylinders such as oscillations of cylinders<sup>8</sup> and their stable modes,<sup>9</sup> the vortex motion above a plane,<sup>10</sup> and an experimental Partial Image Velocimetry (PIV) investigation with dual step cylinders.<sup>11</sup> Similarly, the focus of this application is circular cylinders with the emphasis on the mean-steady flow to use as a benchmark test. For intermediate Reynolds number at values 26 and 36, the NSlet is approximated by an Eulerlet close to its origin and an Oseenlet further away. This reduces to the matched method of Chadwick<sup>12</sup> which shows good comparison to experiment.

Second, consider uniform flow with Reynolds number  $Re \sim 10^6$  past a slender body whose cross section is elliptical and approximate the NSlet by the Eulerlet. It is seen that this is equivalent<sup>5</sup> to the uniform flow past a slender body with an elliptical cross section in Oseen flow given by Chadwick<sup>13</sup> who satisfies the slip body boundary condition for the potential part of the Oseen flow description.

Finally, consider the Blasius problem of uniform flow past a semi-infinite flat plate and take the first three terms in the NSlet expansion. The first of these terms reduces to the Oseen-Blasius solution, which does not predict well the Blasius boundary layer. However, including the next two terms is equivalent to the expansion obtained from a different approach by Kusunawa.<sup>14</sup> In this way, we see that with each term, the Blasius solution is recovered more accurately and the first three terms in the NSlet are sufficient to give a good approximation.

## II. STATEMENT OF THE PROBLEM

We consider time-dependent, incompressible fluid of density  $\rho$ , and viscosity  $\mu$  such that the Navier-Stokes equation

$$\rho \frac{\partial u_i^\dagger}{\partial t^\dagger} + \rho u_j^\dagger \frac{\partial u_i^\dagger}{\partial x_j^\dagger} = -\frac{\partial p^\dagger}{\partial x_i^\dagger} + \mu \frac{\partial^2 u_i^\dagger}{\partial x_j^\dagger \partial x_j^\dagger} \quad (1)$$

and the continuity equation

$$\frac{\partial u_i^\dagger}{\partial x_i^\dagger} = 0 \quad (2)$$

hold throughout the fluid, where the symbol  $\dagger$  denotes dimensional and unperturbed quantities. Fields  $u_i^\dagger$  and  $p^\dagger$  are the fluid velocity and static pressure, respectively, in Cartesian co-ordinates  $x_i^\dagger$ ,  $1 \leq i \leq 2$  for two-dimensional flow, and  $1 \leq i \leq 3$  for three-dimensional flow. Einstein's convention of a repeated suffix implying a summation is used ( $a_i b_i = a_1 b_1 + a_2 b_2 + a_3 b_3$  in three-dimensions, for example).

Consider an exterior problem with a uniform velocity translation such that the far-field boundary condition has the fluid tending toward a uniform stream of magnitude  $U$  aligned along the  $x_1^\dagger$  axis such that

$$u_i^\dagger = U \delta_{i1}, \quad (3)$$

where  $\delta_{ij}$  is Kronecker delta such that  $\delta_{ij} = 1$  when  $i = j$  and  $\delta_{ij} = 0$  otherwise. The normalized perturbed velocity  $u_i$  and (Bernoulli) normalized perturbed pressure  $p$  to the uniform stream satisfy  $u_i^\dagger = U \delta_{i1} + U u_i$ ,  $p^\dagger = -(1/2)\rho U^2 + \rho U^2 p$ , and the normalized co-ordinates are  $x_i^\dagger = l x_i$ ,  $t^\dagger = T t$ . The perturbed Navier-Stokes equation is then

$$St \frac{\partial u_i}{\partial t'} + \frac{\partial u_i}{\partial x_1'} + u_j^j \frac{\partial u_i}{\partial x_j'} = -\frac{\partial p}{\partial x_i'} + (1/Re) \frac{\partial^2 u_i}{\partial x_j' \partial x_j'}, \quad (4)$$

where  $St = l/(UT)$  is the Strouhal number and  $Re = \rho U l / \mu$  is the Reynolds number. We can rewrite (4) as

$$N_i = St u_{i;0} + u_{i;1} + u_j u_{ij} + p_{;i} - (1/Re) u_{i;jj} = 0, \quad (5)$$

where the semicolon represents a derivative with respect to the primed co-ordinates and a derivative with respect to the index 0 means a derivative with respect to time  $t'$  ( $a_{;0} = \frac{\partial a}{\partial t'}$ , for example). In (5), it is implicitly assumed that the velocity and pressure are functions of the primed co-ordinates ( $t', x_i'$ ). In the Green's boundary integral formulation, we denote the variable of integration by the primed co-ordinates. By contrast, the Green's function depends on the variables  $(t - t', x_i - x_i')$ , where the co-ordinate of a point in the fluid is given as  $(t, x_i)$ . Thus, we can designate the  $k$ th NSlet for the velocity as  $u_{ik}(t - t', x_i - x_i')$  and the pressure as  $p_k(t - t', x_i - x_i')$  such that the following equation is satisfied:

$$N_{ik} = St u_{ik;0} + u_{ik;1} + u_{jk^*} u_{ik^*j} + p_{k;i} - (1/Re) u_{ik;jj} = -\delta \delta_{ik}. \quad (6)$$

Here, a comma denotes a derivative with respect to the unprimed co-ordinates (implying  $a_{;j} = -a_{,j}$ ) and the asterisk means no implied summation ( $a_{k^*} a_{k^*} = a_1 a_1$  when  $k = 1$ , for example). The symbol  $\delta$  denotes the Dirac delta function such that  $\int_{\Sigma_\epsilon} \delta d\Sigma = 1$ , where the domain  $\Sigma_\epsilon$  is sufficiently close to and encloses the origin.

Consider the domain  $\Sigma$  in space-time consisting of an exterior domain  $\Sigma_+$  and an interior domain  $\Sigma_-$  to the closed boundary  $\partial\Sigma_0$  over which the velocity is specified. This closed boundary could represent a body in a fluid. Furthermore, consider the exterior domain  $\Sigma_+$  to be bounded by a vanishingly small boundary  $\partial\Sigma_\delta$  around the point  $(t, x_i)$  and a far-field boundary  $\partial\Sigma_\infty$ . The Green's integration over  $(t', x'_i)$  will be taken over the whole of the domain  $\Sigma$  as shown in Fig. 1.

Over the far-field boundary  $\partial\Sigma_\infty$ , we have

$$u_i \rightarrow 0. \tag{7}$$

In addition, the NSlet satisfies

$$\int_{\Sigma_\delta} N_{ik} d\Sigma = \int_{\Sigma_\delta} N_{ijk,J} d\Sigma = \int_{\partial\Sigma_\delta} N_{ijk} n_J d\sigma = - \int_{\Sigma_\delta} \delta\delta_{ik} d\Sigma = -\delta_{ik}, \tag{8}$$

where

$$N_{ijk} = St u_{ik} \delta_{0J} + u_i \delta_{1j} + u_{jk^*} u_{ik^*} + p_k \delta_{ij} - (1/Re) u_{ik,j}, \tag{9}$$

where  $\sigma$  refers to the boundary of the space  $\Sigma$  and  $d\sigma$  is an infinitesimal element on the boundary of the space  $\Sigma$ . The capital index  $J$  is for space-time  $0 \leq J \leq 3$  in the case of 3-dimensional flow, and  $J = 0$  refers to time. The space vector  $a_j = (a_1, a_2, a_3)$  may now be represented in space-time by  $a_j = (a_0, a_1, a_2, a_3)$ , where  $a_0 = 0$ . Therefore, the complementary conjugate integration over primed space is

$$\begin{aligned} \int_{\Sigma_\delta} N_{ik} d\Sigma &= \int_{\Sigma_\delta} N_{ik} d\Sigma' = \int_{\Sigma_\delta} N_{ijk,J} d\Sigma' \\ &= - \int_{\Sigma_\delta} N_{ijk,J} d\Sigma' = - \int_{\partial\Sigma_\delta} N_{ijk} n_J d\sigma', \end{aligned} \tag{10}$$

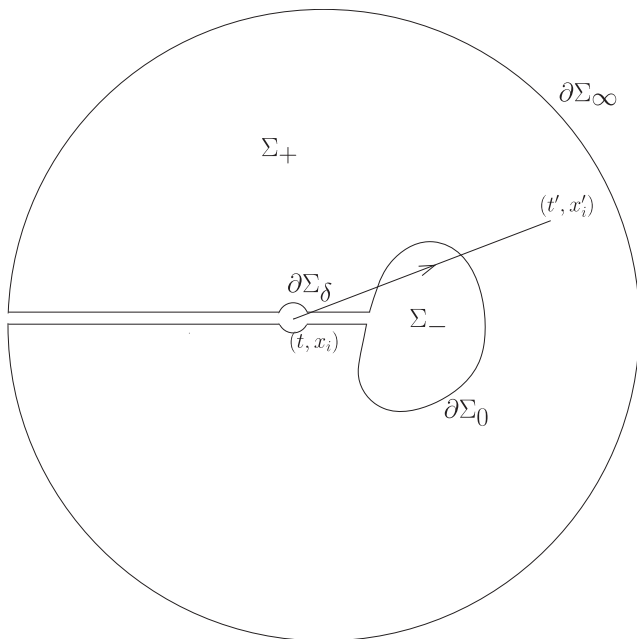


FIG. 1. The domain of integration  $\Sigma$  and its boundaries.

and so

$$\int_{\partial\Sigma_\delta} N_{ijk} n_J d\sigma' = \delta_{ik}. \tag{11}$$

### III. GREEN'S INTEGRAL FORMULATION

Consider the Green's integral formulation of Oseen,<sup>15</sup>

$$\int_{\Sigma} [N_i u_{ik} - N_{ik} u_i] d\Sigma' = 0. \tag{12}$$

The integrand is reformulated as

$$\begin{aligned} N_i u_{ik} - N_{ik} u_i &= (St u_{i;0} + u_{i;1} + u_j u_{ij} + p_{,i} - (1/Re) u_{ijj}) u_{ik} \\ &\quad - (St u_{ik;0} + u_{ik;1} + u_{jk^*} u_{ik^*} + p_{k,i} - (1/Re) u_{ijj}) u_i \\ &= [St u_i u_{ik}]_{;0} + [u_i u_{ik}]_{;1} + [p u_{ik} + p_k u_i]_{;i} \\ &\quad - (1/Re) [u_{ij} u_{ik} - u_{ikj} u_i]_{;j} + [u_{jk^*} u_{ik^*} u_i]_{;j} + Q_k, \end{aligned} \tag{13}$$

where the nonlinear term is

$$Q_k = u_j u_{ij} u_{ik} - u_{ij} u_{jk^*} u_{ik^*}. \tag{14}$$

Consequently,  $Q_k$  may be represented by a potential  $q_{jk}$  such that  $q_{j;k;j} = Q_k$ , where

$$q_{jk} = q_k \hat{r}_j = q_k \cos \theta_j. \tag{15}$$

$\hat{r}_j$  is the unit radial vector in the direction of  $x'_i$  from  $x_i$ , and  $\cos \theta_j = (x'_j - x_j)/r$  with  $r = \sqrt{(x'_1 - x_1)^2 + (x'_2 - x_2)^2}$  in two-dimensions, and  $\cos \theta_j = (x'_j - x_j)/R$  with  $R = \sqrt{(x'_1 - x_1)^2 + (x'_2 - x_2)^2 + (x'_3 - x_3)^2}$  in three-dimensions.

#### A. Definition of $q_k$

We define  $q_k$  as a line integral along a radial spoke such that

$$q_k = \begin{cases} (1/r) \int_0^r r' Q'_k dr', & \text{in two-dimensions,} \\ (1/R^2) \int_0^R R'^2 Q'_k dR', & \text{in three-dimensions.} \end{cases} \tag{16}$$

Hence,  $N_i u_{ik} - N_{ik} u_i = ns_{jk;J}$ , where

$$\begin{aligned} ns_{jk} &= St u_i u_{ik} \delta_{j0} + u_i u_{ik} \delta_{j1} + [p u_{ik} + p_k u_i] \delta_{ij} \\ &\quad - (1/Re) [u_{ij} u_{ik} - u_{ikj} u_i] + u_{jk^*} u_{ik^*} u_i + q_{jk} \\ &= u_i [St u_{ik} \delta_{j0} + u_{ik} \delta_{j1} + u_{jk^*} u_{ik^*} + p_k \delta_{ij} - (1/Re) u_{ik,j}] \\ &\quad - u_{ik} [-p \delta_{ij} + (1/Re) u_{ij}] + q_{jk} \\ &= u_i N_{ijk} - u_{ik} \tau_{ij} + q_{jk}, \end{aligned} \tag{17}$$

and  $\tau_{ij} = -p \delta_{ij} + (1/Re) u_{ij}$  is the stress tensor. So we have

$$\begin{aligned} \int_{\Sigma} [N_i u_{ik} - N_{ik} u_i] d\Sigma' &= \int_{\Sigma} ns_{jk;J} d\Sigma' = \int_{\partial\Sigma} ns_{jk} n_j^\Sigma d\sigma', \\ &= \int_{\partial\Sigma} [u_i N_{ijk} - u_{ik} \tau_{ij} + q_{jk}] n_j^\Sigma d\sigma', \end{aligned} \tag{18}$$

where  $n_j^\Sigma$  is the outward pointing normal to the domain  $\Sigma$ .

### B. Evaluation around $\partial\Sigma_\delta$

Consider translating with the velocity at  $x_i$ ; then, the Stokes equation holds in the vicinity of  $x_i$  represented by the Stokeslets. Equivalently, one might consider that the velocity is, to leading order, the velocity at the fluid point. So locally, the Oseen linearization about this velocity holds, giving the Oseen equations in the vicinity of  $x_i$  represented by the Oseenlets. Sufficiently close to the point, the Oseenlets tend toward the Stokeslets. The NSlet will thus have the same order of magnitude as the Stokeslet in the vicinity of the point. The Stokeslets have order<sup>15</sup>

$$u_{ik} \sim \begin{cases} \ln r, & \text{in two-dimensional steady flow,} \\ 1/R, & \text{in three-dimensional steady flow,} \\ 1/r^*, & \text{in two-dimensional unsteady flow,} \\ 1/(R^* \sqrt{R^*}), & \text{in three-dimensional unsteady flow,} \end{cases} \quad (19)$$

where  $r^* = \sqrt{(t-t')^2 + r^2}$  and  $R^* = \sqrt{(t-t')^2 + R^2}$  are the space-time distance measures for two-dimensional and three dimensional flows, respectively. The orders for the quadratic variation are then

$$Q_k \sim \begin{cases} (\ln r)^2 \\ 1/R^2 \\ 1/r^{*2} \\ 1/(R^{*3}) \end{cases} \quad q \sim \begin{cases} r(\ln r)^2 \\ 1/R \\ 1/r^* \\ 1/(R^{*2}) \end{cases} \quad (20)$$

for two-dimensional steady, three-dimensional steady, two-dimensional unsteady, and three-dimensional unsteady flows, respectively. This leads to the integral contributions

$$\int_{\partial\Sigma_\delta} u_{ik} d\sigma' \sim \begin{cases} r \ln r \rightarrow 0, \\ R^2/R = R \rightarrow 0, \\ r^{*2}/r^* = r^* \rightarrow 0, \\ R^{*3}/(R^* \sqrt{R^*}) = R^{*3/2} \rightarrow 0, \end{cases} \quad (21)$$

$$\int_{\partial\Sigma_\delta} q d\sigma' \sim \begin{cases} (r \ln r)^2 \rightarrow 0, \\ R^2/R = R \rightarrow 0, \\ r^{*2}/r^* = r^* \rightarrow 0, \\ R^{*3}/(R^{*2}) = R^* \rightarrow 0. \end{cases} \quad (22)$$

So, the only nonzero contribution to the evaluation around  $\partial\Sigma_\delta$  comes from

$$\begin{aligned} \int_{\partial\Sigma_\delta} u_i N_{ijk} n_j^\Sigma d\sigma' &= u_i \int_{\partial\Sigma_\delta} N_{ijk} n_j^\Sigma d\sigma' = -u_i \int_{\partial\Sigma_\delta} N_{ijk} n_j d\sigma' \\ &= -u_i \delta_{ik} = -u_k. \end{aligned} \quad (23)$$

### C. Evaluation around $\partial\Sigma_\infty$

In the far-field, the Navier-Stokes equation tends toward the Oseen equation and, accordingly, the NSlets tend toward the Oseenlets; it is known that this far-field integral is zero (see, for example,<sup>16</sup> for the three-dimensional steady case). Equivalently, the only difference in integrands between the Navier-Stokes and Oseen representations is the nonlinear quadratic velocity contribution, which decays faster than the velocity contribution. Since the velocity

contribution decays to zero, then the nonlinear contribution must do so as well.

### D. Velocity representation

Putting these results into (18) while noting that  $u_i$ ,  $N_{ijk}$ , and  $q_{jk}$  are all continuous across the body boundary  $\partial\Sigma_0$  whereas  $\tau_{ij}$  is not necessarily gives a representation for the fluid velocity as

$$\begin{aligned} u_k &= \int_{\partial\Sigma_0} [u_i N_{ijk} - u_{ik} \tau_{ij} + q_{jk}]^+ n_j^\Sigma d\sigma' \\ &\quad + \int_{\partial\Sigma_0} [u_i N_{ijk} - u_{ik} \tau_{ij} + q_{jk}]^- n_j^\Sigma d\sigma' \\ &= \int_{\partial\Sigma_0} -[u_i N_{ijk} - u_{ik} \tau_{ij} + q_{jk}]^+ n_j d\sigma' \\ &\quad + \int_{\partial\Sigma_0} [u_i N_{ijk} - u_{ik} \tau_{ij} + q_{jk}]^- n_j d\sigma' \\ &= \int_{\partial\Sigma_0} [\tau_{ij}^+ - \tau_{ij}^-] u_{ik} n_j d\sigma' = \int_{\partial\Sigma_0} F_i u_{ik} d\sigma', \end{aligned} \quad (24)$$

where  $[\dots]^+$  means the evaluation in the exterior domain,  $[\dots]^-$  means the evaluation in the interior domain, and  $F_i = [\tau_{ij}^+ - \tau_{ij}^-] n_j$ . For the steady case,  $\partial\Sigma_0$  is the body boundary which we denote by  $\partial\Sigma_B$ , and so

$$u_k = \int_{\partial\Sigma_B} F_i u_{ik} d\sigma'. \quad (25)$$

Writing out the function arguments in full, the vector position is given as  $\mathbf{x} = (x_1, x_2, x_3)$  in three-dimensions for example, and so (25) is

$$u_k(\mathbf{x}) = \int_{\partial\Sigma_B} F_i(\mathbf{x}') u_{ik}(\mathbf{x} - \mathbf{x}') d\sigma'. \quad (26)$$

This means that the velocity is represented by a boundary integral distribution of NSlets positioned over the body surface,  $\partial\Sigma_B$  with strength  $F_i(\mathbf{x}')$  for a point  $\mathbf{x}' = (x'_1, x'_2, x'_3)$  on  $\partial\Sigma_B$ . Since the body boundary conditions are given in terms of the velocity on  $\partial\Sigma_B$ , the general problem is solved in terms of a boundary integral representation and discretized by a numerical scheme such as the boundary element method.

For the unsteady case,  $\partial\Sigma_0$  is the space-time boundary which is the body boundary traced out over time and so

$$u_k = \int_{-\infty}^t \left\{ \int_{\partial\Sigma_B} F_i u_{ik} d\sigma' \right\} dt' = u_k|_{t=0} + \int_0^t \left\{ \int_{\partial\Sigma_B} F_i u_{ik} d\sigma' \right\} dt', \quad (27)$$

where  $u_0|_{t=0}$  is the velocity field at time  $t = 0$ . Writing out the function arguments in full, now including time  $t$  and space  $\mathbf{x}$  as  $(t, \mathbf{x})$ , then Eq. (27) is

$$u_k(t, \mathbf{x}) = u_k(0, \mathbf{x}) + \int_0^t \left\{ \int_{\partial\Sigma_B} F_i(t', \mathbf{x}') u_{ik}(t-t', \mathbf{x} - \mathbf{x}') d\sigma' \right\} dt'. \quad (28)$$

This means that the velocity is represented by a boundary integral distribution of NSlets positioned over the body surface,  $\partial\Sigma_B$  with strength  $F_i(t', \mathbf{x}')$  for a point  $\mathbf{x}'$  on the body surface, traced out over time  $t'$  where  $0 \leq t' \leq t$  from an initial condition given at time  $t = 0$ . Since the body boundary conditions are given in terms of the initial

value at  $t = 0$  and the subsequent body boundary position up to time  $t$ , then the general problem is solved in terms of a boundary integral representation, which can then be given by a numerical scheme such as the boundary element method for the space variable and a finite difference method for the time variable.

### E. Pressure representation

Once the problem has been solved for the velocity, then the pressure can subsequently be obtained from the (generalized) Bernoulli equation in the following way. The fundamental theorem of vector calculus means that any vector can be decomposed into a vorticity-free and potential-free part. So, we may write  $u_i = \phi_{;i} + u_i^\omega$ , where  $\phi_{;i}$  is the vorticity-free part and  $u_i^\omega$  is the potential-free part. A word of caution, this representation is equivalent to the Lamb-Goldstein velocity decomposition which has been shown by Chadwick<sup>17</sup> not to necessarily hold everywhere in the field. However, this issue can be overcome by assuming an integral distribution of the Green's functions instead,<sup>17</sup> and this is what we assume here. Similarly, the expression for the fluid head can be written as  $h_i = u_j u_{;ij} = h_{;i} + h_i^\omega$ , where  $h_{;i}$  is the vorticity-free part and  $h_i^\omega$  is the potential-free part. Then, the pressure gradient, which is vorticity-free, is given by the vorticity-free components only in the Navier-Stokes equation (5). Integrating gives

$$p = -St\phi_{;0} - \phi_{;1} - (1/Re)h \tag{29}$$

since  $\phi_{;ij} = 0$  from the continuity equation. In the inviscid Euler case, we have  $h = (1/2)\phi_{;j}\phi_{;j}$  and so in this case the generalized Bernoulli equation (29) reduces to the standard Bernoulli equation. Instead in the viscous case, the head  $h$  is also likely to include the viscous velocity.

### IV. NSlet REPRESENTATION

We give an expansion for the NSlet, and then, use this below to consider some benchmark applications. Far from the point  $(t, x_i)$ , the NSlets  $u_{ik}$  tend toward the Oseenlets  $u_{ik}^0$ . So, in the far-field, the following asymptotic expansion is valid:

$$u_{ik} = u_{ik}^0 + u_{ik}^I + \dots \tag{30}$$

In the above equation, the Oseenlets  $u_{ik}^0$  are known, see, for example, Oseen,<sup>15</sup> and satisfy the Oseenlet equation

$$u_{ik,0}^0 + u_{ik,1}^0 + u_{jk^*}^0 u_{ik^*,j}^0 + p_{k,i}^0 - (1/Re)u_{ik,jj}^0 = -\delta\delta_{ik}. \tag{31}$$

The next term in the expansion then satisfies

$$u_{ik,0}^I + u_{ik,1}^I + u_{jk^*}^I u_{ik^*,j}^I + p_{k,i}^I - (1/Re)u_{ik,jj}^I = -u_{jk^*}^0 u_{ik^*,j}^0, \tag{32}$$

and so on. In this way, we can expand asymptotically near to the point  $(t, x_i)$ , where the NSlets tend toward the Stokeslets. Since the Oseenlets tend toward the same Stokeslets, then the same expansion can be used to represent the expansion sufficiently close to the point. So sufficiently far away and sufficiently close to the point, the NSlets are represented by

$$u_{ik} = \sum_{N=0}^{N=\infty} u_{ik}^N \tag{33}$$

This expression can then be used to continue for the NSlets into the remainder of the domain. In the applications that follow, we approximate the NSlet given in (33) in the following ways: for low Reynolds number, we consider the first term in this expression only, which is the Oseenlet and which itself tends to the Stokeslet for the low Reynolds number; for the high Reynolds number, we consider the Eulerlet which is the high Reynolds number limit of the Oseenlet; for intermediate Reynolds numbers, we consider the NSlet approximated by an Eulerlet in the near-field and an Oseenlet in the far-field; and for boundary layer flow, we consider the first three terms in the NSlet expansion and as well apply the boundary layer approximation.

### V. APPLICATIONS

We consider three problems: (1) flow past a circular cylinder across a variety of Reynolds numbers, (2) flow past a slender body aligned closely to the flow direction at high Reynolds number with elliptical cross section, and (3) boundary layer flow past a semi-infinite flat plate.

#### A. Two-dimensional steady flow past a circular cylinder at low Reynolds number

##### 1. Low Reynolds number flow

Consider using the velocity representation given by (25) in a boundary element numerical scheme such as presented by Dang and Chadwick.<sup>18</sup> In this scheme, the force distribution is approximated by shape functions located at  $n$  nodes on the body boundary such that

$$F_j \approx N_\beta F_{\beta j}, \tag{34}$$

where  $1 \leq \beta \leq n$ , and the repeated index  $\beta$  implies a summation over all  $n$  terms. Under the standard Galerkin scheme,  $n$  weighting functions  $W_\alpha$  are then considered giving the following equations to be solved:

$$\int_{\partial\Sigma_B} W_\alpha u_i d\sigma = \int_{\partial\Sigma_B} W_\alpha \int_{\partial\Sigma_B} N_\beta F_{\beta j} u_{ij} d\sigma' d\sigma, \tag{35}$$

where  $1 \leq \alpha \leq n$ . So

$$u_{\alpha i} = u_{\alpha\beta j} F_{\beta j}, \tag{36}$$

where  $u_{\alpha i} = \int_{\partial\Sigma_B} W_\alpha u_i d\sigma$  and  $u_{\alpha\beta j} = \int_{\partial\Sigma_B} W_\alpha \int_{\partial\Sigma_B} N_\beta u_{ij} d\sigma'$ . Renumbering  $\alpha^* = \alpha + (i - 1)n$  and  $\beta^* = \beta + (j - 1)n$  then gives the matrix equation

$$u_{\alpha^*} = u_{\alpha^*\beta^*} F_{\beta^*}, \tag{37}$$

which can be solved by a dense matrix solver to determine an approximation for the force distribution  $F_i$  at each node  $\beta$  given by  $F_{\beta i}$ .

At the low Reynolds number, the near-field flow tends toward Stokes flow and the far-field flow tends toward Oseen flow. To avoid the Stokes paradox, these two flows must be matched. We note that in the far-field, the NSlets in (25) are approximated by the Oseenlets giving an Oseen flow field approximation in the field far from the body. It is also noted that in the near-field, the Oseenlet approximates to the Stokeslet, giving a Stokes flow field close to the

body. Therefore, approximating the NSlets by the Oseenlets in (25) gives

$$u_k \approx u_k^0 = \int_{\partial\Sigma_B} F_i^0 u_{ik}^0 d\sigma'. \tag{38}$$

This is expected to give a good leading order approximation to the flow field from this theory where  $u_k^0$  is the Oseen velocity approximation,  $F_i^0$  is the force distribution for the two-dimensional steady normalized Oseenlets given by Chadwick<sup>5</sup> as

$$\begin{aligned} u_{i1}^0 &= \frac{1}{2\pi} \left\{ \left[ \ln r + e^{kx_1} K_0(kr) \right]_{,i} - 2ke^{kx_1} K_0(kr) \delta_{i1} \right\}, \\ u_{i2}^0 &= \frac{1}{2\pi} \varepsilon_{ij3} \left[ \ln r + e^{kx_1} K_0(kr) \right]_{,j}, \quad p_k^0 = -\frac{1}{2\pi} [\ln r]_{,k}, \end{aligned} \tag{39}$$

where  $p_k^0$  is the pressure of the  $k$ th Oseenlet. Dang and Chadwick<sup>18</sup> consider this boundary element scheme with collocation point weighting functions, linear shape functions, and logarithmic numerical replacement of the singularity  $u_{ij}^s = \frac{k}{2\pi} \ln r \delta_{ij}$  by its analytic evaluation. The drag coefficient, given by

$$C_D \approx \int_{\partial\Sigma_B} N_\beta F_{\beta 1} d\sigma, \tag{40}$$

is then evaluated and compared against other methods, see Fig. 2. For this range of Reynolds numbers, the new method is closer to experiment than the analyses of Kaplun<sup>6</sup> (asymptotic matching of near-field and far-field representations of the flow at low Reynolds number), Lamb<sup>19</sup> (approximating the form of the Oseen solution), Stokes (slow flow approximation without the treatment of Stokes's paradox), and Tomotika<sup>20</sup> (deploying an expansion formula based on an *ad hoc* use of a distribution of simple solutions in Oseen and Euler flow). From existing theory, this is unexpected because, classically, Oseen flow is valid when the linearization to a uniform flow field holds. Such an assumption is violated close to the circular cylinder and is true only in the far field. However, from this new theory,

it is expected, as the Oseenlet is a leading order linearization of the NSlet. The results given in Fig. 2 demonstrate good agreement with experiment which therefore supports the theory.

### 2. High Reynolds number flow

In the high Reynolds number limit, it is shown in the work of Chadwick<sup>7</sup> that the NSlet  $u_{ik}$  approximates to the Eulerlet  $u_{ik}^E$  given by

$$u_{i1}^E = \frac{1}{2\pi} [\ln r]_{,i} - H(x_1) \delta(x_2) \delta_{i1}, \quad u_{i2}^E = -\frac{1}{2\pi} [\theta]_{,i} \tag{41}$$

where  $H(x_1)$  is the heaviside function and  $\theta$  is the polar angle. Therefore, for high Reynolds number flow, (25) becomes

$$u_k \approx u_k^E = \int_{\partial\Sigma_B} F_i^E u_{ik}^E d\sigma', \tag{42}$$

where  $u_k^E$  is the Euler velocity generated by an integral distribution of Eulerlets given by  $u_{ik}^E$  with strength  $F_i^E$ . Equation (42) is also given in Chadwick<sup>5</sup> but by a different derivation involving a matching between near-field Euler flow and far-field Oseen flow. It is shown by Chadwick<sup>5</sup> that (42) provides an accurate model. As an example, we see a close relation to the pressure distribution over a circular cylinder surface in uniform flow for both subcritical laminar flow ( $Re \sim 10^6$ ) and turbulent flow ( $Re \sim 10^7$ ), given in Fig. 3. The characteristic features of the physics of the flow such as reversal in the pressure gradient at an angle of around  $70^\circ - 80^\circ$ , and a negative flattened pressure profile in the wake of the cylinder are reproduced. Hence, the theory presented in this paper is consistent with an Eulerlet model and matches well to experiments.<sup>21</sup>

### 3. Reynolds number 26 and 36

This time, in (25), the NSlets are approximated by Eulerlets in the near-field and Oseenlets in the far-field, and the two flows are

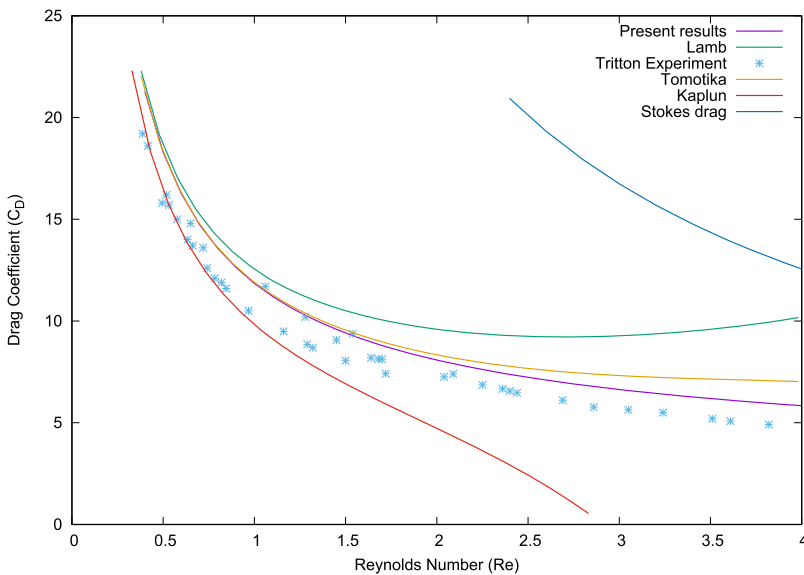
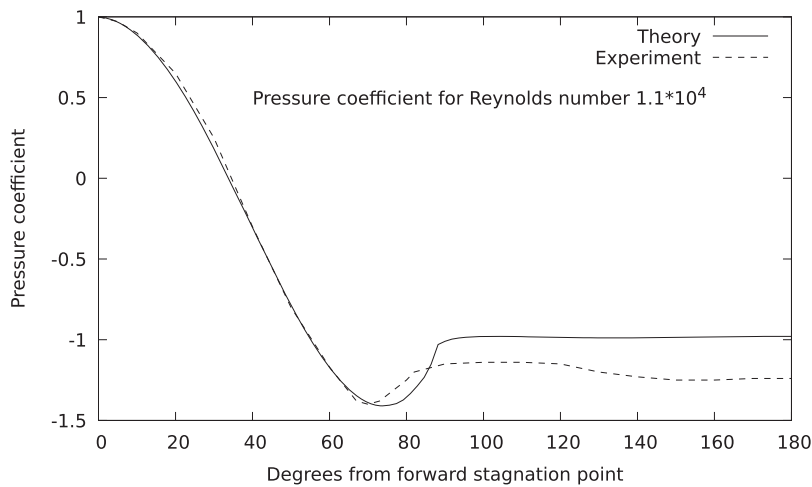
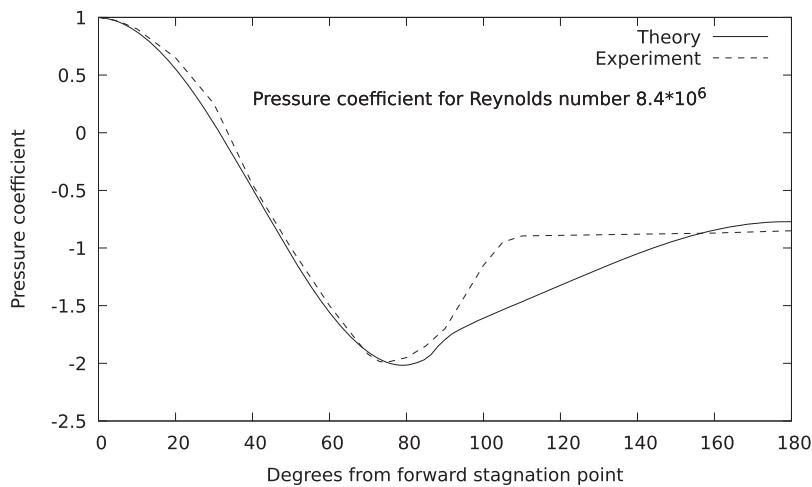


FIG. 2. Comparison of drag coefficient against Reynolds number.<sup>18</sup>



(a)



(b)

**FIG. 3.** Pressure distribution comparison between the theory of Chadwick<sup>5</sup> and the experiment reproduced with permission from Batchelor (*An Introduction to Fluid Dynamics*. Copyright 1967 Cambridge University Press.)<sup>21</sup> (a) for subcritical laminar flow and (b) for turbulent flow.

merged for a smooth transition (within the radius range  $1 \leq r \leq 6$  such that at  $r = 1$  the flow is purely Euler and at  $r = 6$  the flow is purely Oseen). A cosine distribution of Eulerlets is considered. Even though the theoretical approach is markedly different, it is equivalent to the description given by Chadwick *et al.*<sup>12</sup> considering a near-field Euler flow matched to a far-field Oseen flow. From this, the following results are then obtained for laminar flow at Reynolds number 26 given in Fig. 4, and 36 given in Fig. 5. Comparing the flow fields in Fig. 4, we note that the separation point is closely matched, and the size and the shape of the eddies are reproduced. Therefore, it is seen that, given the approximations made, good agreement is obtained with the experiment.

We also present experimental results for the far-field decay at Reynolds number  $Re = 36$  from Kovasznay.<sup>22</sup> Comparing the wake cross sections with the theory, we note that the trend in diffusion is captured, the general wake profile is captured, and so there is again good agreement.

### B. Two-dimensional steady flow past a slender body with elliptical cross section at high Reynolds number

This case is a reproduction of previous work<sup>13</sup> on Oseen flow theory. At high Reynolds numbers close to the body, Oseen flow theory is seemingly inconsistent because of the requirement to satisfy the body boundary condition. Despite this, the Oseen theory appears to be a significant improvement over inviscid flow slender body theory<sup>23</sup> and over Jorgensen’s theory,<sup>24</sup> see Fig. 6. The experiments for this comparison were conducted in a low speed wind tunnel at a Reynolds number of around  $Re = 10^6$ . The new theory presented in this paper explains why this should be the case: the Oseenlet is the leading order approximation to the NSlet, and so substituting into (25) gives Oseen flow such that

$$u_k = \int_{\partial\Sigma_B} F_i u_{ik} d\sigma' \approx \int_{\partial\Sigma_B} F_i^0 u_{ik}^0 d\sigma' = u_k^0. \tag{43}$$

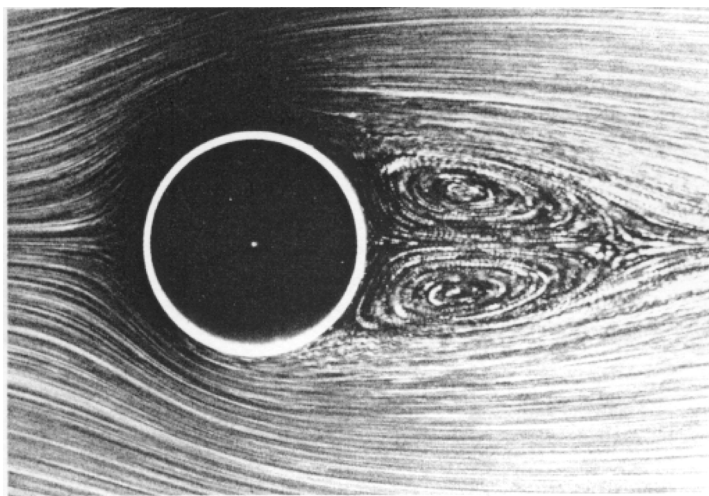
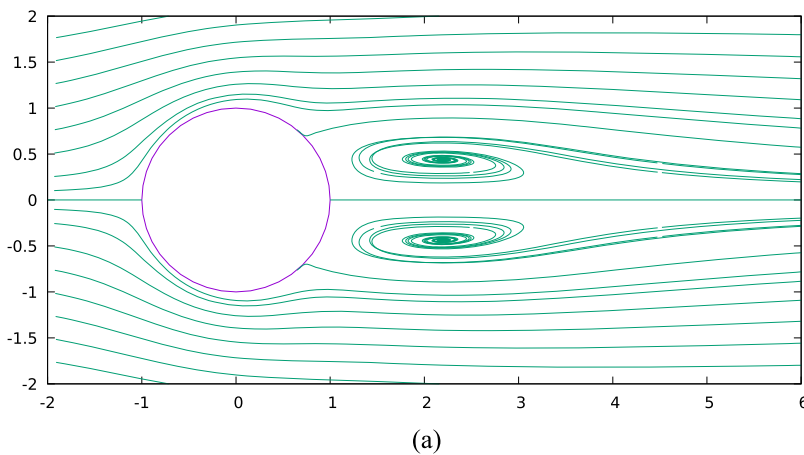


**FIG. 4.** The streamline flow around a steady two-dimensional circular cylinder at Reynolds number  $Re = 26$ . (a) Calculation from the theory of Chadwick *et al.*<sup>12</sup> (b) An image from the experiment belonging to the estate of Professor Sadatoshi Taneda. From Van Dyke, *Album of Fluid Motion*. Copyright Dr. Sadatoshi Taneda. Reprinted with permission from Dr. Hiroshi Taneda.

(b)

Furthermore, in the high Reynolds number limit, the Oseenlet tends toward the Eulerlet; in addition, we have

$$u_k^0 = \int_{\partial\Sigma_B} F_i^0 u_{ik}^0 d\sigma' \approx \int_{\partial\Sigma_B} F_i^E u_{ik}^E d\sigma' = u_k^E. \quad (44)$$

Figure 6 shows that the slender body theory in Oseen flow<sup>13</sup> gives a close match to experiment for the lift  $L$ . Here, ellipticity  $e$  is defined as the ratio of the semiminor axis to the semimajor axis  $s$  of the ellipse cross section and  $\alpha$  is the angle of attack. Again, from existing theory, this is surprising as the Oseen flow approximation is violated on the surface of the slender body. However, from this new theory it is expected as the Oseenlet is a leading order linearization of the NSlet.

### C. Boundary layer flow past a semi-infinite flat plate

In this section, we introduce new theory to describe the Green's function fundamental solution in boundary layer flow, and we call this new function the BL-let. This is then used to describe the flow

by applying the boundary layer approximation and considering terms in Eq. (33). We begin by considering only the first term in (33). However, it is seen that this is not accurate in describing the flow, and so two more subsequent terms are included. Following the method of Kusunaka,<sup>14</sup> it is shown that an accurate description is obtained.

In the boundary layer, the Navier-Stokes equations approximate to the boundary layer equations<sup>25</sup> given by

$$v_j v_{1,j} + v_{1,1} - (1/Re)v_{1,22} = 0, \quad (45)$$

where  $v_i$  is the boundary layer velocity. Therefore, the approximation to the NSlet in the boundary layer satisfies

$$v_{j1} v_{11,j} + v_{11,1} - (1/Re)v_{11,22} = -\delta, \quad (46)$$

where  $v_{jk}$  is the BL-let. So, in the boundary layer, (25) becomes

$$u_k \approx v_k = \int_{\partial\Sigma_B} G_i v_{ik} d\sigma', \quad (47)$$

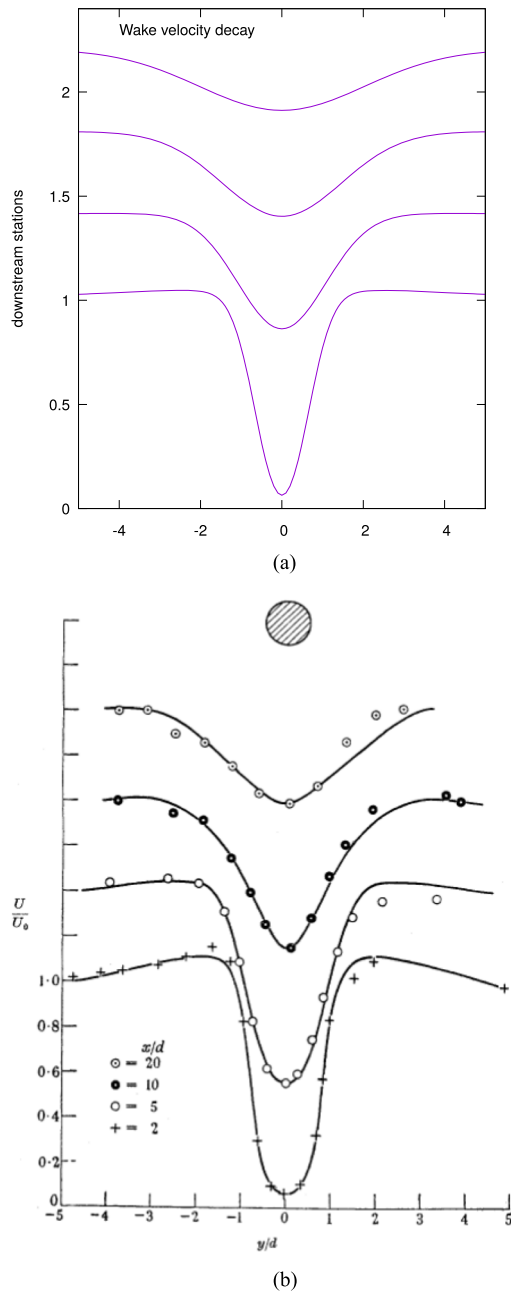


**FIG. 5.** Axial wake velocity for flow around a steady two-dimensional circular cylinder at Reynolds number  $Re = 36$ , taken at downstream wake cross sections positioned at distances 2, 5, 10, and 20 times the diameter. (a) Calculated from the theory of Chadwick *et al.*<sup>12</sup> (b) Reproduced from the experiments of Kovanszay [“Hot-wire investigation of the wake behind cylinders at low Reynolds numbers,” Proc. R. Soc. London, Ser. A **198**, 174–190 (1949). Copyright 1949 The Royal Society].<sup>22</sup>

where  $G_i$  is an approximation of the force distribution  $F_i$  in the boundary layer. The body boundary lies along the infinite half line, and the symmetry of the problem means that there is only an axial force so that

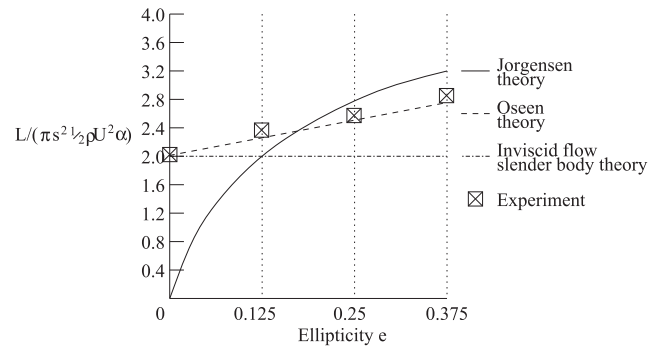


**FIG. 6.** Comparison of lift between Oseen theory, inviscid potential flow theory, and Jorgensen theory against the experiment for a slender body with an elliptic cross section.<sup>13</sup>

$$v_k = \int_0^\infty G_1 v_{1k} dx'_1. \tag{48}$$

We now seek  $v_{ik}$  by first looking at the leading-order description.

**1. Leading-order term**

Consider the leading order term in (33), which is the Oseen approximation to the boundary layer Green’s function solution, given by

$$v_{11,1}^0 - (1/Re)v_{11,22}^0 = -\delta. \tag{49}$$

We can use Fourier Transforms to evaluate this. Integrating through (49) with the Fourier integral for both the  $x_1$  and  $x_2$  variables gives

$$\int_{-\infty}^\infty \int_{-\infty}^\infty (v_{11,1}^0 - (1/Re)v_{11,22}^0) e^{-i\omega_1 x_1} e^{-i\omega_2 x_2} dx_1 dx_2 = - \int_{-\infty}^\infty \int_{-\infty}^\infty \delta(x_1)\delta(x_2) e^{-i\omega_1 x_1} e^{-i\omega_2 x_2} dx_1 dx_2 = -1 \tag{50}$$

for the Fourier Transform variables  $\omega_1$  and  $\omega_2$ . So using standard Fourier Transform theory for differentials, we have

$$i\omega_1 \bar{v} - (1/Re)(\omega_2)^2 \bar{v} = 1, \tag{51}$$

where  $\bar{v}$  is the double Fourier Transform of  $v_{11}$ . Therefore,

$$\bar{v} = - \frac{1}{(\omega_2^2/Re) + i\omega_1}. \tag{52}$$

Using the inverse transform  $F^{-1}\{1/(a + i\omega_1)\} = H(x_1)e^{-ax_1}$  then gives the single Fourier transform of  $v_{11}$ ,  $\tilde{v}$ , to be

$$\tilde{v} = -H(x_1)e^{-\omega_2^2 x_1/(Re)}. \tag{53}$$

Applying a second inverse transform

$$F^{-1}\{1/\sqrt{2a}e^{-\omega_2^2/(4a)}\} = \frac{e^{-ax_1^2}}{\sqrt{2\pi}}$$
 then gives

$$v_{11}^0 = - \frac{H(x_1)}{\sqrt{2\pi}} \sqrt{\frac{Re}{2x_1}} e^{-\eta^2}. \tag{54}$$

Here,  $\eta = \sqrt{Re/(4x_1)}x_2$  is the boundary layer variable. Since  $v_{11}^0 = \psi_{2,2}^0$ , the streamfunction is

$$\psi^0 = -\frac{Re}{4\pi x_1} \int_0^{x_2} e^{-\eta'^2} dx_2' = -\frac{1}{\sqrt{\pi}} \int_0^\eta e^{-\eta'^2} d\eta' = -(1/2)\text{erf } \eta. \tag{55}$$

From (48), we then have for the  $x_1$  component of velocity

$$v_1^0 = \int_0^\infty G_1^0 v_1^0 dx_1' = \int_0^{x_1} G_1^0 \Psi_{,2}^0 dx_1', \tag{56}$$

where  $G_1^0$  is the leading-order approximation of the force distribution  $G_1$  and  $v_1^0$  is the leading-order component of the boundary layer velocity. Therefore, the streamfunction  $\Psi^0$  for this flow is given by

$$\Psi^0 = \int_0^{x_1} G_1^0 \psi^0 dx_1' = \int_0^{x_1} G_1^0 (-(1/2)\text{erf } \eta^*) dx_1', \tag{57}$$

where  $\eta^* = \sqrt{\frac{Re}{4x_1^2}} x_2$ ,  $x_1^* = x_1 - x_1'$ . The variable change  $q = x_1'/x_1$  gives

$$\Psi^0 = x_1 \int_0^1 G_1^0(x_1 q) (-(1/2)\text{erf}(\eta/\sqrt{1-q})) dq. \tag{58}$$

However, we know<sup>25</sup> from the self-similarity of the problem given in the standard Blasius approach that  $\Psi^0 = \sqrt{x_1} f(\eta)$  for some function  $f(\eta)$ . Therefore, to get the appropriate variation in  $x_1$ , it must be that  $G_1^0(x_1) = a/\sqrt{x_1}$  for some constant  $a$ . So,

$$\Psi^0 = \int_0^{x_1} (a/\sqrt{x_1'}) (-(1/2)\text{erf } \eta^*) dx_1'. \tag{59}$$

From this result, an expression for the  $x_2$  component of velocity can be calculated. Differentiating (59) with respect to  $x_1$  gives

$$\begin{aligned} v_2^0 &= -\Psi_{,1}^0 = (a/\sqrt{x_1}) ((1/2)\text{erf}(\infty)) - \int_0^{x_1} (a/\sqrt{x_1'}) \\ &\quad \times (-(1/2)\text{erf } \eta^*)_{,1} dx_1' \\ &= (1/2)(a/\sqrt{x_1}) - (1/2) \int_0^{x_1} (a/\sqrt{x_1'}) (\text{erf } \eta^*)_{,1} dx_1' \\ &= (1/2)(a/\sqrt{x_1}) - (1/2) \int_\eta^\infty (a/\sqrt{x_1'}) (\text{erf } \eta^*)_{,\eta^*} d\eta^*. \end{aligned} \tag{60}$$

Here, for a function  $f(x_1 - x_1')$ , we have defined  $f_{,1'} = \frac{\partial f}{\partial x_1'}$ , and so  $f_{,1'} = -f_{,1}$ . Now consider the variable  $q^2 = \eta^{*2} - \eta^2$ , then  $q/\eta^* = \sqrt{x_1'}/\sqrt{x_1}$  and  $d\eta^* = \sqrt{x_1'}/\sqrt{x_1} dq$ , giving

$$\begin{aligned} v_2^0 &= (1/2)(a/\sqrt{x_1}) - (1/2)(a/\sqrt{x_1}) \int_0^\infty \frac{2}{\sqrt{\pi}} e^{-\eta^{*2}} dq \\ &= \frac{a}{2\sqrt{x_1}} (1 - e^{-\eta^2}). \end{aligned} \tag{61}$$

To find  $v_1^0$ , recall that this velocity satisfies

$$v_{1,1}^0 - (1/Re)v_{1,22}^0 = 0, \tag{62}$$

from the continuity equation,  $v_{1,1}^0 = -v_{2,2}^0$ . Substituting into (62) and integrating with respect to  $x_2$  while ensuring that the solution decays gives

$$v_1^0 = \sqrt{Re} \frac{\sqrt{\pi}}{2} a (\text{erf } \eta - 1). \tag{63}$$

The boundary condition on the flat plate is that  $v_1^0 = -1$ , and so  $a = \frac{\sqrt{2}}{\sqrt{(Re)\pi}}$  giving

$$v_1^0 = \text{erf } \eta - 1, \tag{64}$$

and therefore,

$$v_2^0 = \frac{(1 - e^{-\eta^2})}{\sqrt{(Re)\pi x_1}}. \tag{65}$$

This solution is well-known because it has also been calculated by an entirely different method by Burgers<sup>26</sup> and is called the Oseen-Blasius solution. For comparison, Burgers' method is given in the Appendix. Unfortunately, this solution gives a large discrepancy for the stress and so is not sufficiently accurate to be useful. However, the expectation is that if more terms in the expansion for the NSlet given by Eq. (33) are considered, then there will be greater accuracy. So, to enable a more accurate description, we consider additional terms in the expansion.

### 2. Higher-accuracy description

Consider further terms in the velocity expansion of the boundary layer Green's function BL-let,

$$v_{ik} = v_{ik}^0 + v_{ik}^I + v_{ik}^{II} + \dots \tag{66}$$

Substituting into (46) then gives

$$\begin{aligned} (v_{j1}^0 + v_{j1}^I + v_{j1}^{II} + \dots)(v_{i1,j}^0 + v_{i1,j}^I + v_{i1,j}^{II} + \dots) + v_{11,1}^0 + v_{11,1}^I + v_{11,1}^{II} + \dots \\ - (1/Re)(v_{11,22}^0 + v_{11,22}^I + v_{11,22}^{II} + \dots) = -\delta. \end{aligned} \tag{67}$$

Rearrange such that

$$\begin{aligned} v_{11,1}^0 - (1/Re)v_{11,22}^0 &= -\delta \\ v_{11,1}^I - (1/Re)v_{11,22}^I &= -v_{j1}^0 v_{11,j}^0 \\ v_{11,1}^{II} - (1/Re)v_{11,22}^{II} &= -v_{j1}^I v_{11,j}^I - v_{j1}^0 v_{11,j}^0 \\ v_{11,1}^{N-1} - (1/Re)v_{11,22}^{N-1} &= -\sum_{I=0}^{N-2} v_{j1}^I v_{11,j}^{N-I-2}. \end{aligned} \tag{68}$$

Considering  $M$  terms in the expansion and integrating (68) such that

$$v_1^N = \int_0^{x_1} G_1^M v_{11}^N dx_1' \tag{69}$$

gives

$$\begin{aligned} v_{1,1}^0 - (1/Re)v_{1,22}^0 &= 0, \\ v_{1,1}^I - (1/Re)v_{1,22}^I &= -\int_0^{x_1} G_1^M v_{j1}^0 v_{11,j}^0 dx_1', \\ v_{1,1}^{II} - (1/Re)v_{1,22}^{II} &= -\int_0^{x_1} G_1^M (v_{j1}^I v_{11,j}^I - v_{j1}^0 v_{11,j}^0) dx_1', \\ v_{1,1}^{N-1} - (1/Re)v_{1,22}^{N-1} &= -\int_0^{x_1} G_1^M \sum_{I=0}^{N-2} v_{j1}^I v_{11,j}^{N-I-2} dx_1'. \end{aligned} \tag{70}$$

Integrating (66) in the same way gives

$$v_k = v_k^0 + v_k^I + v_k^{II} + \dots \tag{71}$$

Substituting this expansion into (45) gives

$$\begin{aligned} (v_j^0 + v_j^I + v_j^{II} + \dots)(v_{i,j}^0 + v_{i,j}^I + v_{i,j}^{II} + \dots) + v_{1,1}^0 + v_{1,1}^I + v_{1,1}^{II} + \dots \\ - (1/Re)(v_{1,22}^0 + v_{1,22}^I + v_{1,22}^{II} + \dots) = -\delta. \end{aligned} \tag{72}$$

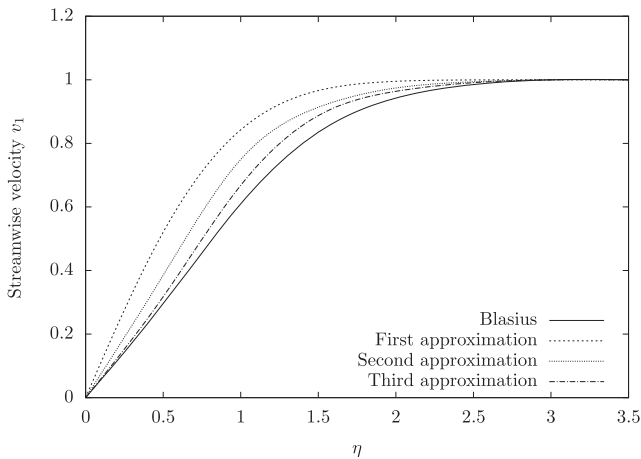


**FIG. 7.** The boundary layer velocity calculated from various approximations to the boundary layer Green's function given by Kusakawa.<sup>14</sup>

Rearranging gives

$$\begin{aligned}
 v_{1,1}^0 - (1/Re)v_{1,22}^0 &= 0, \\
 v_{1,1}^I - (1/Re)v_{1,22}^I &= -v_j^0 v_{1,j}^0, \\
 v_{1,1}^{II} - (1/Re)v_{1,22}^{II} &= -v_j^0 v_{1,j}^I - v_j^I v_{1,j}^0, \\
 v_{1,1}^{N-1} - (1/Re)v_{1,22}^{N-1} &= -\sum_{l=0}^{N-2} v_j^l v_{1,j}^{N-l-2}.
 \end{aligned}
 \tag{73}$$

Comparing (70) and (73), the left-hand side of each equation is the same and so the right-hand sides of each must equal each other.

It is seen that (73) is identical to the expansion given by Kusakawa *et al.*<sup>14</sup> who finds the first three terms. These terms indicate that the expansion converges toward the exact boundary layer solution. However, Kusakawa *et al.* obtain their iteration method by considering an Oseen linearization of the flow field. While this will hold in the far-boundary-layer close to the uniform stream, there is no evidence that it will converge to the boundary layer solution throughout the flow field. Therefore, there is no theoretical justification from Kusakawa that the expansion holds close to the boundary. Instead, we see that from the theory presented here, there is an expectation that the iteration method will converge to the exact boundary layer solution, and the numerical results reproduced from Ref. 14 in Fig. 7 indicate this.

## VI. CONCLUSION

A new method is given which represents the incompressible Navier-Stokes velocity by a linear boundary integral distribution of Navier-Stokes Green's functions which we call NSlets for both the steady and unsteady problem in two- and three-dimensional flows. The NSlets are determined and given in terms of an infinite series with the first term being the respective Oseenlets.

The representation is the same for both exterior and interior flow problems. The strength of the NSlets is given by the stress tensor and so is the fluid force acting on the boundary. In the near-field for low Reynolds number, the NSlets tend toward Stokeslets and

so the Stokes flow velocity representation<sup>2,3</sup> is recovered. Similarly, for Oseen flow, the NSlets become Oseenlets and the Oseen flow velocity representation<sup>4,15</sup> is recovered. In the high Reynolds number limit, the NSlets tend toward Eulerlets and the Euler flow velocity representation<sup>5</sup> is recovered.

Given this representation, a problem which stipulates the velocity on the body boundary is then easily solved in a straightforward manner, in the same way as for Oseen and Stokes flow problems. Once the velocity is found, then the solution can be put back into the equations in order to determine the pressure. Therefore, this represents a general linearized solution to the incompressible Navier-Stokes problem by a Green's integral distribution of Green's functions.

Three two-dimensional benchmark problems are considered, uniform flow past a circular cylinder, a slender body with elliptical cross section, and a semi-infinite flat plate. For the first two problems, the first term (Oseenlet) is given to approximate the NSlet. For high Reynolds number, this is further approximated by the Eulerlet. For the final problem, the first three terms are considered and the boundary layer approximation is applied. For all cases, good agreement with benchmark results are found.

This gives explanation to Shankar's observation<sup>2</sup> that the Oseen flow representation is a surprisingly good model given the body boundary condition violation. The explanation is that the fluid velocity is represented by an integral distribution of NSlets and the leading order approximation to the NSlet is the Oseenlet, and so an Oseen flow model is a leading order representation of the flow for these problems.

Future work is to model applications across the Reynolds number range by developing a boundary element code for this boundary integral representation. Rather than using the first few terms in the expansion for the NSlets, a numerical scheme will be used to determine more accurately the full NSlet which can then be fed into the boundary element code.

## ACKNOWLEDGMENTS

I would like to acknowledge the support of my family and friends. In particular, I would like to acknowledge Dr. Thurai Rahulan and Dr. James Christian from the University of Salford for helping proof read the manuscript.

## NOMENCLATURE

$\rho, \mu, U, l, T$	dimensional parameters: density, coefficient of viscosity, uniform stream velocity, typical body length, and typical time period
$Re = \rho Ul/\mu$	dimensionless Reynolds number
$St = l/(UT)$	dimensionless Strouhal number
superscript †	dimensional variable: Navier-Stokes
$\mathbf{u}^\dagger, p^\dagger, \mathbf{x}^\dagger$	velocity, pressure, and position vector
$\mathbf{u}, p$	dimensionless Navier-Stokes velocity and pressure perturbed to a uniform stream
$\mathbf{v}$	dimensionless Boundary Layer velocity perturbed to a uniform stream
$\mathbf{x}$	dimensionless position vector
$\mathbf{x}'$	variable of integration in the Green's integral of the dimensionless position vector

$r$	dimensionless radial length in two dimensions
$r^*$	dimensionless length in two dimensional space-time
$R$	dimensionless radial length in three dimensions
$R^*$	dimensionless length in three dimensional space-time
$a_j$	vector representation with index starting from 1 and ending at dimension of space
$a_j$	vector representation with index starting from 0 with $a_0$ the time co-ordinate
$a_{,i}$	differentiation of $a$ with respect to $x_i$
$a_{,i}$	differentiation of $a$ with respect to $x'_i$
$Q_k$	nonlinear quadratic term in Green's integral
$q_{jk}$	potential of $Q_k$
$\Sigma, d\Sigma$	a region of space, an element of the space
$\partial\Sigma$	the boundary of the region of space
$d\sigma$	an element of the boundary
$\delta$	dirac delta function
$\delta_{ij}$	Kronecker delta

**APPENDIX: BURGERS BOUNDARY LAYER APPROACH**

We follow the method of Burgers<sup>26</sup> who assumes Oseen flow in the boundary layer by an axial distribution of Oseenlets given by

$$u_k \approx u_k^0 = \int_0^\infty F_1^0 u_{1k}^0 dx'_1, \tag{A1}$$

where  $F_1^0$  is the strength of the drag Oseenlets  $u_{k1}^0 = u_{1k}^0$  lying along the positive  $x_1$  axis. This representation has been considered by Olmstead<sup>4</sup> who finds a solution by using the Wiener-Hopf technique.<sup>27</sup> However, Olmstead omits a few key proofs and a complete detailed analysis is given in Darghoth.<sup>28</sup> The Wiener-Hopf technique then gives the force distribution as

$$F_1^0 = \frac{2}{\sqrt{(Re)\pi x_1}}. \tag{A2}$$

In the boundary layer, this can be further approximated. Letting the ratio of  $x_1/x_2$  become large in the downstream boundary layer, Adamu and Chadwick<sup>29</sup> show that the drag Oseenlet approximates to Imai's far-field drag expression.<sup>30</sup> Equivalently, Burgers<sup>26</sup> also approximates the Oseenlet, and in both cases the solution in the boundary layer is given by

$$\begin{aligned} u_{11}^0 \approx v_{11}^0 &= \psi_2^0 \\ u_{21}^0 \approx v_{21}^0 &= -\psi_1^0 \\ \psi^0 &= -(1/2)\operatorname{erf}\eta + (1/(2\pi))\theta, \end{aligned} \tag{A3}$$

where  $\eta = \sqrt{Re/(4x_1)}x_2$  is the boundary layer variable and  $\theta$  is the polar angle. [We note in this formulation the term  $(1/(2\pi))\theta$  is required in the representation of  $\psi^0$  whereas in the derivation in Sec. V C it is not. This is because here we give the velocity  $v_2^0$  representation first directly from the integral (A4) given next, whereas in Sec. V C we give the streamfunction  $\Psi^0$  representation first for which the term  $(1/(2\pi))\theta$  is lower order and so can be ignored. The velocity  $v_2^0$  is then determined from this.] Substituting this into (A1) gives an expression for the transverse boundary layer velocity component  $v_2^0$  as

$$u_2^0 \approx v_2^0 = \int_0^\infty F_1^0 v_{21}^0 dx'_1. \tag{A4}$$

The term  $(1/(2\pi))\theta$  in  $\psi^0$  from Eq. (A3) represents a line of two-dimensional Laplacian sources, and an integral distribution of these with strength given by (A2) is given, for example, in Darghoth.<sup>28</sup> By using the substitutions for the integral variable from  $x'_1$  to  $\eta^*$ , where  $\eta^* = \sqrt{\frac{Re}{4x_1^*}}x_2$ ,  $x_1^* = x_1 - x'_1$ , and then to  $q$  where  $q^2 = \eta^{*2} - \eta^2$ , the integral in (A4) is calculated, see Burgers<sup>26</sup> and Darghoth.<sup>28</sup> This gives

$$v_2^0 = \frac{(1 - e^{-\eta^2})}{\sqrt{(Re)\pi x_1}}. \tag{A5}$$

From this, the axial streamwise velocity can be calculated, for example, in the same way as given in Sec. V C.

**REFERENCES**

- <sup>1</sup>E. Chadwick, "A boundary integral velocity representation of the steady Navier-Stokes equations for a body in an exterior domain uniform flow field," in *Advances in Boundary Element and Meshless Techniques XIX* (EC Ltd Publications, Eastleigh, UK, 2018), pp. 97–101.
- <sup>2</sup>P. Shankar, *Slow Viscous Flows* (Imperial College Press, London, UK, 2007).
- <sup>3</sup>C. Pozrikidis, *Fluid Dynamics* (Springer, USA, 2009).
- <sup>4</sup>W. Olmstead and A. Gautesen, "Integral representations and the Oseen flow problem," in *Mechanics Today* (Pergamon Press, New York, 1976), Vol. 3, pp. 125–189.
- <sup>5</sup>E. Chadwick, J. Christian, A. Kapoulas, and K. Chalasani, "The theory and application of Eulerlets," *Phys. Fluids* **31**, 047106 (2019).
- <sup>6</sup>S. Kaplun and P. Lagerstrom, "Low Reynolds number flow past a circular cylinder," *J. Math. Mech.* **6**, 595–603 (1957).
- <sup>7</sup>H. Yano and A. Kieda, "An approximate method for solving two-dimensional low-Reynolds-number flow past arbitrary cylindrical bodies," *J. Fluid Mech.* **97**, 157–179 (1980).
- <sup>8</sup>T. Sengupta and D. Patidar, "Flow past a circular cylinder executing rotary oscillation: Dimensionality of the problem," *Phys. Fluids* **30**, 093602 (2018).
- <sup>9</sup>H. Jiang, L. Cheng, F. Tong, S. Draper, and H. An, "Stable state of mode A for flow past a circular cylinder," *Phys. Fluids* **28**, 104103-1–104103-13 (2016).
- <sup>10</sup>G. Vasconcelos and M. Moura, "Vortex motion around a circular cylinder above a plane," *Phys. Fluids* **29**, 083603 (2017).
- <sup>11</sup>C. Morton, S. Yarusyevych, and F. Scarano, "A tomographic PIV investigation of the flow development over dual step cylinders," *Phys. Fluids* **28**, 025104 (2016).
- <sup>12</sup>E. Chadwick, J. Christian, and K. Chalasani, "Using eulerlets to model steady uniform flow past a circular cylinder," *Eur. J. Comput. Mech.* **27**, 469–478 (2018).
- <sup>13</sup>E. Chadwick, "Experimental verification of an Oseen flow slender body theory," *J. Fluid Mech.* **654**, 271–279 (2010).
- <sup>14</sup>K. Kusakawa, S. Suwa, and T. Nakagawa, "An iteration method to solve the boundary layer flow past a flat plate," *J. Appl. Math. Phys.* **2**, 35–40 (2014).
- <sup>15</sup>C. Oseen, *Neue Methoden und Ergebnisse in der Hydrodynamik* (Akademische Verlagsgesellschaft, Leipzig, 1927).
- <sup>16</sup>N. Fishwick and E. Chadwick, "The evaluation of the far-field integral in the Green's function representation for steady Oseen flow," *Phys. Fluids* **18**, 113101-1–113101-5 (2006).
- <sup>17</sup>E. Chadwick, "The far field Oseen velocity expansion," *Proc. R. Soc. London, Ser. A* **54**, 2059–2082 (1998).
- <sup>18</sup>B. Dang and E. Chadwick, "BEM for low Reynolds number flow past a steady circular cylinder in an unbounded domain," in UKBIM12 Conference Proceedings, 2019.
- <sup>19</sup>H. Lamb, *Hydrodynamics* (Cambridge University Press, Cambridge, 1932).
- <sup>20</sup>S. Tomotika and T. Aoi, "An expansion formula for the drag on a circular cylinder moving through a viscous fluid at small Reynolds numbers," *Q. J. Mech. Appl. Math.* **4**, 401–406 (1951).

- <sup>21</sup>G. Batchelor, *An Introduction to Fluid Dynamics* (Cambridge University Press, Cambridge, 1967).
- <sup>22</sup>L. G. Kovasznay, “Hot-wire investigation of the wake behind cylinders at low Reynolds numbers,” *Proc. R. Soc. London, Ser. A* **198**, 174–190 (1949).
- <sup>23</sup>M. Lighthill, “Note on the swimming of slender fish,” *J. Fluid Mech.* **9**, 305–317 (1960).
- <sup>24</sup>L. Jorgensen, “Elliptic cones alone and with wings at supersonic speeds,” National Advisory Committee for Aeronautics Report No. 1376, 1957.
- <sup>25</sup>I. Sobey, *Introduction to Interactive Boundary Layer Theory* (Oxford University Press, Oxford, UK, 2000).
- <sup>26</sup>“Hydrodynamics—On the application of Oseen’s theory to the determination of the friction experienced by an infinitely thin flat plate,” in *Selected Papers of J. M. Burgers*, edited by F. Nieuwstadt and J. Steketee (Springer, Dordrecht, 1995), pp. 134–142.
- <sup>27</sup>B. Noble, *Methods Based on the Wiener-Hopf Technique for the Solution of Partial Differential Equations* (Pergamon Press, New York, 1958).
- <sup>28</sup>R. Darghoth, “An investigation of the Oseen differential equations for the boundary layer,” Ph.D. thesis, University of Salford, Salford, UK, 2018.
- <sup>29</sup>H. Adamu and E. Chadwick, “The leading order equivalence of Oseen’s and Imai’s representations,” in UKBIM12 Conference Proceedings, 2019.
- <sup>30</sup>I. Imai, “On the asymptotic behaviour of viscous fluid flow at a great distance from a cylindrical body, with special reference to Filon’s paradox,” *Proc. R. Soc. A* **208**, 487–516 (1951).